ADCONIP 2014 Hiroshima

Comparison of Semi-Active Suspension Controllers

Alexandro Ortiz-Espinoza[1], Juan Carlos Tudón-Martínez, Ruben Morales-Menendez and Ricardo Ramirez-Mendoza

***Abstract*— Two hybrid control algorithms, Sky Hook-Ground Hook and Mix-1-Sensor, were tested in an automotive semi-active suspension. A commercial Magneto-Rheological damper was implemented using an Artificial Neural Network in a Quarter of Vehicle model. The automotive semi-active suspension was implemented in a commercial *Controller Area Network* system; the control algorithms were implemented in an *Arduino Due* micro-controller system. Early results show better performance than automotive passive system and the feasibility of this application in a commercial vehicle.**

I. Introduction

Automotive suspension system has important goals: isolate the vehicle chassis from road disturbances and keep in contact the wheel and the road. These objectives could be performed simultaneously in a semiactive suspension system by modifying the damping coefficient.

The key variables in a semi-active automotive suspension control system are the velocity and vertical acceleration of the sprung and unsprung mass, [1]. This control system consists of sensors, actuators, and an *Electronic Control Unit* (*ECU*) communicated through a shared bus such as the *Controller Area Network* (*CAN*). *CAN* framework stablishes a standard for efficient and reliable real-time communications between these components, [2].

An experimental platform using an *Axiomatic*$^{\text{TM}}$*CAN* was implemented for this research. A *Quarter of Vehicle* (*QoV*) model with a *Magneto Rheological* (*MR*) damper were embedded in a *cRIO* of *National Instruments*$^{\text{TM}}$to mimic in real-time the semi-active suspension behavior. An *Arduino* micro-controller hosts the control algorithms.

This paper is organized as follows: in section II the *MR* damper model is briefly described. Section III presents the experimental set up. Section IV discusses the results. And, section V concludes this paper.

II. MR damper modeling

Since the *MR* damper is the key device, an accurate model is needed. Two major frameworks have been established for *MR* damper modeling: parametric and non-parametric equations. The parametric models describe the physical phenomena in mathematical expressions, [3]. The non-parametric models, [4], are an alternative to represent this phenomena, without considering a *priori* knowledge with no physical meaning such as the *Artificial Neural Networks* (*ANN*) framework.

The main advantages of the *ANN*-based framework are the simplicity of structure, extrapolation capability, simple identification algorithm and, low number of parameters.

Two major groups of *ANN* architectures have been considered. *Feedforward* networks project the flow of information only in one way; while, *recurrent* networks have an output feedback signal used as an internal memory into the network. The *recurrent* network has a memory of the immediately past events that affect the adjustment of the *weights* in all layers; thus, the learning algorithm can improve the modeling performance by using the same data set used in a *feedforward* network. However, this advantage has a considerable cost, the processing time is increased.

A commercial *MR* damper, manufactured by *Delphi MagneRide*$^{\text{TM}}$was used, [5]. It has continuous actuation with high deflections. Its range of force is $\pm 4,000$ N, with 40 mm of stroke and time constant of 15 ms.

An *MTS-407*$^{\text{TM}}$controller has been used to control the position of the damper piston. An *NI-9172*$^{\text{TM}}$data acquisition system commands the controller and records the position, velocity and force from the *MR* damper. A sampling frequency of 1,650 Hz was used. The frequency band of displacement is 0.5 - 15 Hz, which lies in automotive applications. The displacement and electric current ranges are: ± 25 mm and (0 - 2.5) A, respectively.

To obtain the simplest *ANN*-based model control system, ten replicas of each experiment were used to evaluate statistically the modeling results; for each replica, 60 % of the data were used in the learning phase and the remainder in the testing phase. The *ANN* architecture (2 input, 10 hidden, and 1 output neurons) has been chosen to represent the *MR* damper dynamics. The proposed *ANN*-based model has been intensively validated with different experimental tests that explore all phenomena of the *MR* damper.

Modeling results of the proposed *ANN* model, present a median of 6 % and mean of 7.2 % of error. The *ANN* model is capable to reproduce the changes of the experimental force. To validate the capability of modeling the nonlinear phenomena of the *MR* damper, experimental data are compared with the *ANN*-based model in the characteristic diagram of *Force-Velocity* (*FV*), [5].

III. Experimental System

The *Axiomatic*$^{\text{TM}}$*CAN* based platform consists of: 4 *Analog Input* (*AI*) modules, 4 *Analog Output* (*AO*) modules,

*This work was supported by the *Tecnológico de Monterrey* (*Autotronics* research chair) and *CONACyT* (*PCP* 03/10)

[1]A. Ortiz-Espinoza, J.C. Tudón-Martínez, R. Morales-Menendez and R. Ramírez-Mendoza are with the Tecnologico de Monterrey {A00787745, A00287756, rmm, ricardo.ramirez} @itesm.mx

2 inclinometers. The bandwidth of the *CAN* bus was 250 kbits/s, Fig. 1.

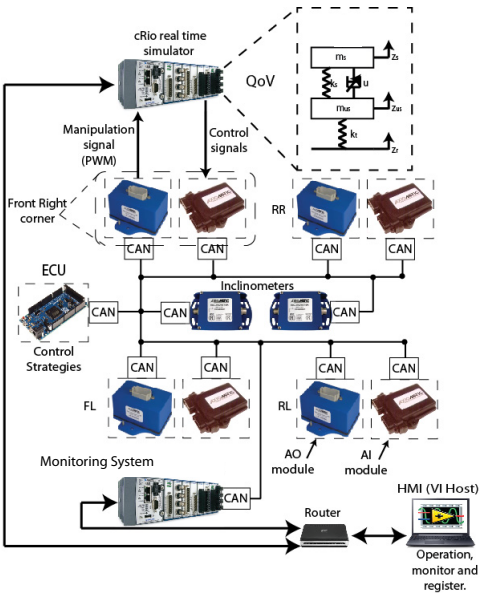

Fig. 1. Experimental System.

A classical *QoV* model was used, because the aim of the analysis was the vertical dynamic of suspension, Fig. 2. This model describes the vertical behavior of a vehicle according to the suspension; it was implemented into a *Real Time Simulator cRIO*. The model is described by:

$$\begin{aligned} m_s\ddot{z}_s &= -F_D - k_s z_s \\ m_{us}\ddot{z}_{us} &= k_s z_s + F_D - k_t(z_{us} - z_r) \end{aligned} \tag{1}$$

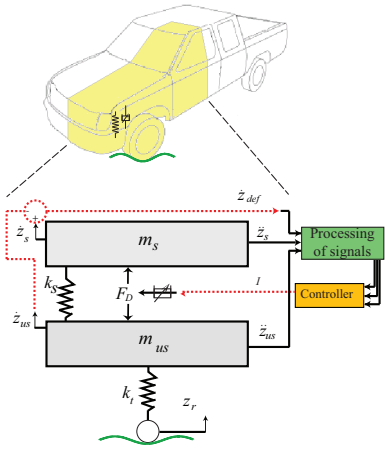

Fig. 2. Quarter of Vehicle (QoV) model.

The state-space representation of this system is:

$$\dot{x} = Ax + Bu \tag{2}$$

$$y = Cx + Du \tag{3}$$

$$A = \begin{bmatrix} 0 & -\frac{k_s}{m_s} & 0 & \frac{k_s}{m_s} \\ 1 & 0 & 0 & 0 \\ 0 & \frac{k_s}{m_{us}} & 0 & -\frac{k_s+k_t}{m_{us}} \\ 0 & 0 & 1 & 0 \end{bmatrix} \quad B = \begin{bmatrix} -\frac{1}{m_s} & 0 \\ 0 & 0 \\ \frac{1}{m_{us}} & \frac{k_t}{m_{us}} \\ 0 & 0 \end{bmatrix}$$

$$C = \begin{bmatrix} 0 & 1 & 0 & -1 \\ 1 & 0 & 0 & 0 \\ 0 & 0 & 1 & 0 \\ 0 & -\frac{k_s}{m_s} & 0 & \frac{k_s}{m_s} \\ 0 & \frac{k_s}{m_{us}} & 0 & -\frac{k_s+k_t}{m_{us}} \end{bmatrix} \quad D = \begin{bmatrix} 0 & 0 \\ 0 & 0 \\ 0 & 0 \\ -\frac{1}{m_s} & 0 \\ \frac{1}{m_{us}} & \frac{k_t}{m_{us}} \end{bmatrix}$$

where $\dot{x} = [\dddot{z}_s \ \ddot{z}_s \ \dot{z}_{us} \ \ddot{z}_{us}]^T$, $x = [\ddot{z}_s \ \dot{z}_s \ z_s \ \dot{z}_{us} \ z_{us}]^T$, $u = [F_D \ z_r]^T$ $y = [z_{def} \ \ddot{z}_s \ \dot{z}_{us} \ \dot{z}_s \ \ddot{z}_{us}]^T$; $\ddot{z}_s$, $\dot{z}_s$ and z_s are the acceleration, velocity and position of the sprung mass; $\ddot{z}_{us}$, $\dot{z}_{us}$ and z_{us} are for the unsprung mass. F_D is the damper force and z_r is the road profile. The parameters for this *QoV* model were: $m_s = 517.2$ kg, $m_{us} = 81.5$ kg, $k_s = 45,000$ N/m, and $k_t = 230,000$ N/m. This model was discretized with a 200 Hz frequency and embedded into a *cRio* 9014 of *National Instruments*™. The *cRio* 9014 had two modules: (1) *AO* module and (2) *DI* module. The signals sent by the *AO NI* module were: $\dot{z}_s$, $\ddot{z}_s$, $\dot{z}_{us}$ and $\ddot{z}_{us}$, all in the range of 0 – 5 V. The *AI* module received the four signals and it samples all inputs every 10 ms. The *DI NI* module received the *PWM* signal sent by *AO* module with a frequency of 20 kHz and 0 – 100 % duty cycle.

The *Electronic Control Unit* (*ECU*) was implemented in a *Arduino Due* micro-controller as an embedded control system. A transceiver *Texas Instrument*™, one on each port, was used to perform the communication between *ECU* and *CAN*.

The most representative control algorithm for comfort is the *Sky-Hook* (*SH*) controller, [6]. The principle of this approach is to *link* the chassis to the *sky* by a virtual damper and put a controlled damper among the masses in order to reduce the vertical oscillations of the chassis. The *SH* algorithm has two-states:

$$c_{sky} = \begin{cases} c_{min} & \text{if} \quad \dot{z}_s(\dot{z}_s - \dot{z}_{us}) \leq 0 \\ c_{max} & \text{if} \quad \dot{z}_s(\dot{z}_s - \dot{z}_{us}) > 0 \end{cases} \tag{4}$$

where c_{min} is the minimum damping coefficient in a semi-active damper and c_{max} its counterpart. Some improvements to the *SH* controller have been proposed, such as the adaptive c_{sky} in [7], the gain-scheduling c_{sky} in [8] and continuous adaptation to the c_{sky} in [9]. Based on the acceleration measurement instead of the velocity of the sprung mass, the named *Acceleration Driven Damper* (*ADD*) control and its improved version, *SH-ADD* control, [10] have become efficient comfort-oriented controllers. In the sense of reducing the number of measurements that are used to control the damping force, [11] proposed the *Mix-1-Stroke* control strategy that shows similar performance as the *SH-ADD* controller but with only one measurement. Its control law is:

$$c_{Mix1} = \begin{cases} c_{max} & \text{if} \quad (\ddot{z}_s^2 - \nu^2\dot{z}_s^2) \leq 0 \\ c_{min} & \text{if} \quad (\ddot{z}_s^2 - \nu^2\dot{z}_s^2) > 0 \end{cases} \tag{5}$$

where ν is the cut-off frequency in the frequency response of the sprung mass acceleration of the *QoV* model, between the low and high damping curve.

In a dual way to the *SH*, the *Ground-Hook* (*GH*)algorithm has been proposed to reduce the road holding [12] by including a virtual damping between the wheel and road and a controllable semi-active shock absorber, whose damping coefficient is given by:

$$c_{GH} = \begin{cases} c_{min} & \text{if} \quad -\dot{z}_{us}(\dot{z}_s - \dot{z}_{us}) \leq 0 \\ c_{max} & \text{if} \quad -\dot{z}_{us}(\dot{z}_s - \dot{z}_{us}) > 0 \end{cases} \tag{6}$$

To manage the compromise between comfort and road holding with data-based controllers, [13] propose a hybrid control strategy that weights the *SH* and *GH* control outputs, according to:

$$c_{hybrid} = \lambda c_{SH} + (1 - \lambda) c_{GH} \tag{7}$$

where λ is a parameter of design used to weight the comfort and road holding performances; it can be optimized by using the trade-off curve, Fig. 7. Based on this previous idea two

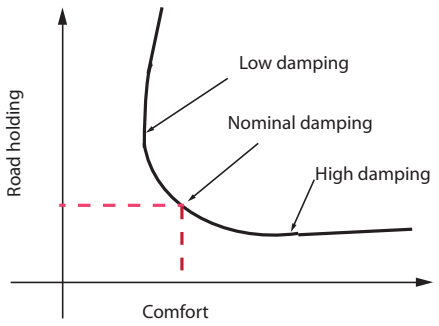

Fig. 3. Trade-off performance criteria for a suspension.

control algorithms were implemented in the *ECU*:

(1) Hybrid *Sky-Hook and Ground-Hook* (*SHGH*) [6], [12]:

$$F_{Hybrid} = \lambda F_{SH} + (1 - \lambda) F_{GH} \tag{8}$$

where F_{SH} is:

$$F_{SH} = \begin{cases} c_{min}(\dot{z}_s - \dot{z}_{us}) & \text{if} \quad \dot{z}_s(\dot{z}_s - \dot{z}_{us}) \leq 0 \\ c_{SH}\dot{z}_{us} & \text{if} \quad \dot{z}_s(\dot{z}_s - \dot{z}_{us}) > 0 \end{cases} \tag{9}$$

and F_{GH} is:

$$F_{GH} = \begin{cases} c_{min}(\dot{z}_s - \dot{z}_{us}) & \text{if} \quad -\dot{z}_{us}(\dot{z}_s - \dot{z}_{us}) \leq 0 \\ c_{GH}\dot{z}_{us} & \text{if} \quad -\dot{z}_{us}(\dot{z}_s - \dot{z}_{us}) > 0 \end{cases} \tag{10}$$

(2) The hybrid *Mix-One-Sensor* (*M1S*), [14]:

$$C_{M1S-c} = \begin{cases} c_{max} & \text{if} \quad (\ddot{z}_s^2 - \alpha^2 \dot{z}_s^2) \leq 0 \\ c_{min} & \text{if} \quad (\ddot{z}_s^2 - \alpha^2 \dot{z}_s^2) > 0 \end{cases} \tag{11}$$

$$C_{M1S-rh} = \begin{cases} c_{max} & \text{if} \quad (\ddot{z}_s^2 - \alpha^2 \dot{z}_s^2) > 0 \\ c_{min} & \text{if} \quad (\ddot{z}_s^2 - \alpha^2 \dot{z}_s^2) \leq 0 \end{cases} \tag{12}$$

where C_{M1S-c} and C_{M1S-rh} are the coefficients for comfort and road holding; $\alpha = 2\pi f$ where f is the frequency of change between passive (c_{min}) and active (c_{max}).

Two types of road were implemented to test the performance of controllers: (1) a road profile and (2) a *Boggs* type surface. The road profile mimics a rough runway surface according on standard ISO-8606:1995; while, the *Boggs* type surface is a sine wave with a decreasing amplitude (30 - 0 mm) and increasing frequency (0.5 - 30 Hz). This signal allows to explore the resonance of sprung mass and unsprung masses, [15].

IV. Results

To evaluate the different control algorithms, the *pseudo-Bode* diagram and *Power Spectral Density* of the key variables were exploited to show the performance in different frequency bands. The mathematical definitions for comfort and road holding are, [16]:

- *Comfort* is measured with the vertical chassis acceleration ($\ddot{z}_s$) response to road disturbances (z_r), between 0 and 20 Hz. This is the acceleration felt by the passengers.
- *Road holding* is measured with the vertical wheel deflection ($z_{us} - z_r$) response to road disturbances (z_r), between 0 to 30 Hz. It represents the ability of the wheel to stay in contact with the road.

The common goal is the minimization of either the energy transfer from z_r to $\ddot{z}_s$ (comfort), or the energy transfer from z_r to $(z_{us} - z_r)$ (road holding) or a tradeoff of these two energy transfers over a frequencies bands. Four frequency bands (*FB*) are defined based on the resonance frequencies of the masses of the *QoV* model, [17]:

1) FB_1: [0-2] Hz range, the goal is comfort. People can feel dizziness and motion sickness. This bandwidth includes the resonance frequency of the sprung mass, typically in 1-2 hz.
2) FB_2: [2-9] Hz range, the goal is comfort. High gains of vertical accelerations generate an overall discomfort.
3) FB_3: [9-16] Hz range, the goal is road holding. It contains the unsprung mass frequency resonance into the 10-15 Hz, affecting the road holding and increasing the discomfort.
4) FB_4: [16-20] Hz range, the goal is road holding. Dangerous vibration of the head with respect to shoulders could generate internal damage.

Figure 4 summarizes an analysis of hybrid algorithms. These plots correspond to pseudo-*Bode* of (A) displacement and (B) acceleration of sprung mass, (C) displacement of unsprung mass and (D) deflection of suspension. Left plots are for *SHGH* algorithm with different λ (0.0, 0.2, 0.5, 0.8, 1.0) and right plots are for *M1S* algorithm. When λ = 1 the main goal is comfort, if λ = 0 the main goal is road holding; any value in between is a trade off of these goals. These results validate the performance in the different frequency bands.

Figure 5 shows the *Power Spectral Density* (*PSD*) of the different performance variables under the frequency band of comfort goal [0-6] Hz (left plots) and road holding goal [6-12] Hz (right plots) for each hybrid control algorithm. These

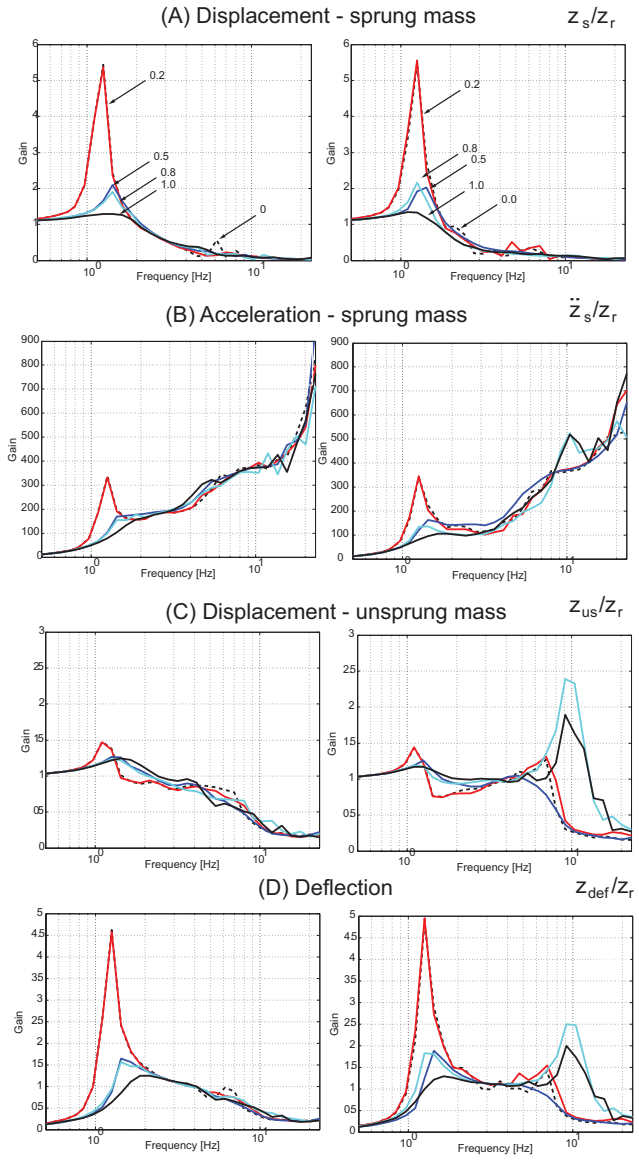

Fig. 4. Pseudo-Bode of hybrid controllers using different λ. Left plots correspond to *SHGH* algorithm; rigth plots to *M1S* algorithm

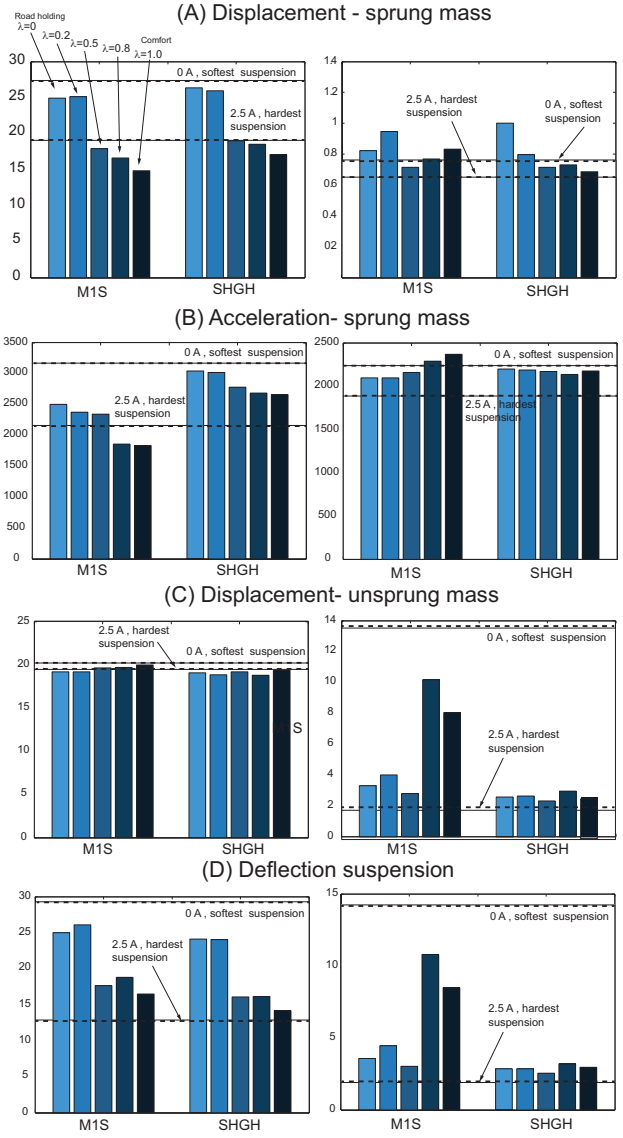

Fig. 5. *PSD* plots of hybrid controllers using different λ.

plots also include the softest suspension (*0 A*) and the hardest suspension (*2.5 A*) condition as a reference point (dashed lines).

The *M1S* control algorithm oriented to comfort (λ = 1.0) has lower *PSD* than *SHGH* algorithm in the frequency band of comfort, 5(A,B left). However, *SHGH* control algorithm (λ = 0.5) has lower *PSD* than *M1S* algorithm in the frequency band of road holding, Fig. 5(C,D rigth).

A comparison of both hybrid algorithms is shown in Fig. 6 based on pseudo-*Bode* plots. The suspension performance in the passive extreme conditions: softest (0 A) and hardest (2.5 A) were included.

Both control algorithms reduce the acceleration and displacement gain response around the sprung mass resonance (1 - 2 Hz), Figs. 6(A,B), this improves the comfort. But, around frequency band of road holding (6 - 12 Hz) increases considerably the gain. In Figs. 6(C,D) *SHGH* reduces displacement responses around the unsprung mass resonance, but *M1S* had a high gain in road holding frequency ($\sim$ 10 Hz).

Both control algorithms have a better performance than the passive suspension in the extreme conditions for both goals: comfort and road holding. There is a great opportunity the implementation of these ideas in a vehicle using *CAN* system. Using a common-bus, as *CAN*, instead of point-to-point approach, introduces different forms of time delay uncertainty between sensors, actuators, and controllers. The characteristics of time delays could be constant, bounded, or even random, depending on the network protocols, [18]. Time delay could drastically reduce the performance, a better study is needed, [19].

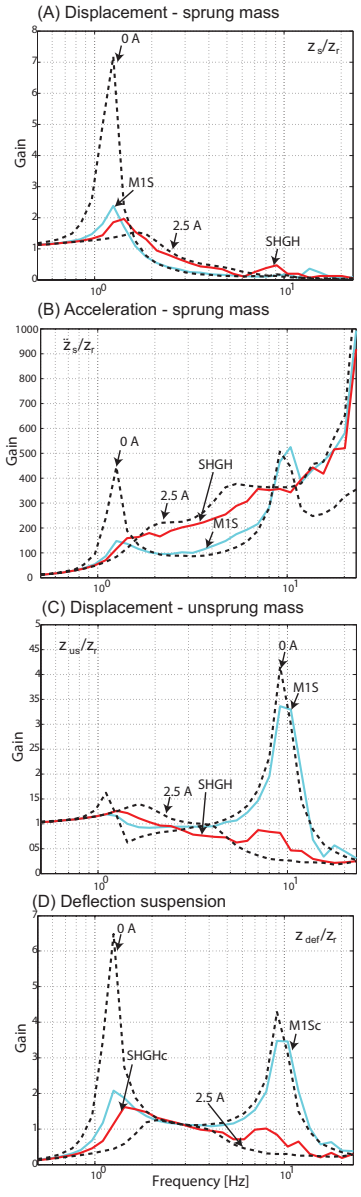

Fig. 6. Comparision of hybrid control algorithms using pseudo-Bode plots.

V. Conclusions

Two control algorithms were tested with a *Quarter of Vehicle* (*QoV*) model: *hybrid Sky Hook and Ground Hook* (*SHGH*), and *hybrid Mix-One-Sensor* (*M1S*). A commercial *Magneto-Rheological* (*MR*) damper was implemented using an Artificial Neural Network based approach. The automotive semi-active suspension was implemented in a commercial *CAN* based system; the control algorithm were implemented into an *Arduino Due* micro-controller system.

Comfort and road holding were the main goals of semi-active suspension system. These goals were evaluated with some performance indexes based on pseudo-*Bode* diagram and *Power Spectral Density* of the key variables: acceleration and displacement of the sprung mass for comfort and displacement and deflection of the unsprung mass for road holding. Two types of road were implemented in the frequency bands domain to compare the control algorithms: a road profile and a *Boggs* type surface. Results show the feasibility of this commercial application. All control algorithms have better results than the standard solutions (i.e. softest or hardest suspension system).

References

[1] E. Wang, X. Qing, S. Rakheja, and C. Su, "Semi-active Control of Vehicle Vibration with MR-dampers," in *IEEE Conf. on Decision and Control*, 2003, pp. 2270–2275.

[2] R. Li, C. Liu, and F. Luo, "A Design for Automotive CAN Bus Monitoring System," in *IEEE Conf. on Vehicle Power and Propulsion*, 2008, pp. 1–5.

[3] L. Wang and H. Kamath, "Modeling Hysteretic Behaviour in MR Fluids and Dampers using Phase-Transition Theory," *Smart Mater. Struct.*, vol. 15, pp. 1725–1733, 2006.

[4] K. Ahn, M. Islam, and D. Truong, "Hysteresis Modeling of Magneto-Rheological (MR) Fluid Damper by Self Tuning Fuzzy Control," in *ICCAS 2008, Seoul Korea*, 2008, pp. 2628–2633.

[5] J. Tudon-Martinez, R. Morales-Menendez, R. Ramirez, and L. G.-C. non, "MR Damper Identification using ANN based on 1-Sensor A Tool fo Semi-Active Suspension Control Compliance," in 4^{th} *Int Conf on Neural Computation Theory and Applications*, Spain, Oct 2012, pp. 493–502.

[6] D. Karnopp, M. Crosby, and R. Harwood, "Vibration Control Using Semi-Active Force Generators," *Trans. of ASME, J. of Eng. for Industry*, vol. 96, pp. 619–626, 1974.

[7] R. Kim and K. Hong, "Skyhook Control Using a Full-Vehicle Model and Four Relative Displacement Sensors." in *Int. Conf. on Control, Automation and Systems*, Seoul Corea, 2007.

[8] K. Hong, H. Sohn, and J. Hedrick, "Modified Skyhook Control of Semi-Active Suspensions: A New Model, Gain Scheduling, and Hardware-in-the-Loop Tuning," *ASME Trans. J. of Dynamic Systems, Measurement, and Control*, vol. 124, pp. 158–167, 2002.

[9] K. Yi and B. Song, "A New Adaptive Sky-Hook Control of Vehicle Semi-Active Suspensions," *Proc. IMechE Part D: J. of Automobile Engineering*, vol. 213, pp. 293–303, 1999.

[10] S. Savaresi and C. Spelta, "Mixed Sky-hook and ADD: Approaching the Filtering Limits of a Semi-active Suspension," *ASME Trans.: J. of Dynamic Systems, Measurement and Control*, vol. 169, no. 4, pp. 382–392, 2007.

[11] C. Spelta, "Design and Applications of Semi-Active Suspension Control Systems," Ph.D. dissertation, Politecnico de Milano, 2008.

[12] M. Valasek, M. Novak, Z. Sika, and O. Vaculin, "Extended Ground-Hook – New Concept of Semi-Active Control of Truck Suspension," *Vehicle Syst. Dyn.*, vol. 29, pp. 289–303, 1997.

[13] M. Ahmadian, "A Hybrid Semiactive Control for Secondary Suspension Applications," in *ASME-ICE, Symp. on Advanced Automotive Tech.*, USA, 1997, pp. 743–750.

[14] S. Savaresi and C. Spelta, "A Single-Sensor Control Strategy for Semi-Active Suspensions," *IEEE Trans. on Control Systems Technology*, vol. 17, no. 1, pp. 143 – 152, 2009.

[15] C. Boggs, L. Borg, and J. Ostanek, "Efficient Test Procedures for Characterizing MR Dampers," in *ASME Int. Mechanical Eng. Congress and Exposition*, 2006.

[16] C. Poussot-Vassal, C. Spelta, O. Sename, S. Savaresi, and L. Dugard, "Survey and Performance Evaluation on Some Automotive Semi-Active Suspension Control Methods: A Comparative Study on a Single-Corner Model," *Annual Reviews in Control*, vol. 36, no. 1, pp. 148–160, 2012.

[17] D. Bastow, G. Howard, and J. Whitehead, *Car Suspension and Handling*. Society of Automotive Engineers, 4^{th} Ed., 2004.

[18] F. Lian, J. Moyne, and D. Tilbury, "Network Protocols for Networked Control Systems," in *Handbook of Networked and Embedded Control Systems*, D. Hristu-Varsakelis and W. Levine, Eds. New York: Birkhuser Boston, 2005, pp. 651–675.

[19] A. Ortiz-Espinoza, A. Cabello-Ortega, J. Tudón-Martínez, D. Hernández-Alcantara, and R. Morales-Menendez, "Analysis of On/Off Controllers of a Semi-Active Suspension in CAN," in *to appear in* 19^{th} *IFAC World Congress*, South Africa, 2014.